Enhancing NeRF akin to Enhancing LLMs: Generalizable NeRF Transformer with Mixture-of-View-Experts

Wenyan Cong[1]*, Hanxue Liang[2,1]*, Peihao Wang[1], Zhiwen Fan[1], Tianlong Chen[1],
Mukund Varma[3,1], Yi Wang[1], Zhangyang Wang[1]
[1]University of Texas at Austin, [2]University of Cambridge, [3]Indian Institute of Technology Madras
{wycong, peihaowang, zhiwenfan, tianlong.chen, panzer.wy, atlaswang}@utexas.edu,
hl589@cam.ac.uk, mukundvarmat@gmail.com

Abstract

*Cross-scene generalizable NeRF models, which can directly synthesize novel views of unseen scenes, have become a new spotlight of the NeRF field. Several existing attempts rely on increasingly end-to-end "neuralized" architectures, i.e., replacing scene representation and/or rendering modules with performant neural networks such as transformers, and turning novel view synthesis into a feedforward inference pipeline. While those feedforward "neuralized" architectures still do not fit diverse scenes well out of the box, we propose to bridge them with the powerful Mixture-of-Experts (MoE) idea from large language models (LLMs), which has demonstrated superior generalization ability by balancing between larger overall model capacity and flexible per-instance specialization. Starting from a recent generalizable NeRF architecture called GNT [53], we first demonstrate that MoE can be neatly plugged in to enhance the model. We further customize a shared permanent expert and a geometry-aware consistency loss to enforce cross-scene consistency and spatial smoothness respectively, which are essential for generalizable view synthesis. Our proposed model, dubbed GNT with Mixture-of-View-Experts (**GNT-MOVE**), has experimentally shown state-of-the-art results when transferring to unseen scenes, indicating remarkably better cross-scene generalization in both zero-shot and few-shot settings. Our codes are available at https://github.com/VITA-Group/GNT-MOVE.*

1. Introduction

Given several images from different viewpoints, Neural Radiance Field (NeRF) has achieved remarkable success on synthesizing novel views. Most existing methods [34, 31, 41, 61, 14, 51, 3, 64, 65, 22] focus on overfitting one single scene by reconstructing its 3D radiance field

in a "backward" manner. Though capable of generating realistic and consistent novel views, the need for retraining on each new scene limits their practical applications. Recently, generalizable NeRF has settled a new trend: in place of the costly per-scene fitting, several pioneer works [70, 58, 69, 53, 49] attempt to synthesize novel views of unseen scenes in a "feedforward" fashion on the fly. Those models are first pre-trained by learning how to represent scenes and render novel views from captured images across different scenes, achieving high-quality "zero-shot" inference results on new scenes. Among them, Generalizable NeRF Transformer (GNT) [53] stands out by replacing the explicit scene modeling and rendering function via unified, data-driven, and scalable transformers, and automatically inducing multi-view consistent geometries and renderings via large-scale novel view synthesis pre-training.

However, those cross-scene NeRF models face the fundamental dilemma between **"generality"** and **"specialization"**. On the one hand, they need to broadly cover both diverse scene representations and/or rendering mechanisms due to different scene properties (*e.g.*, color, materials) – hence larger overall model size is needed to guarantee sufficient expressiveness. On the other hand, since a single scene usually consists of specialized self-similar appearance patterns, those models must also be capable of per-scene specialization to model the scene closely. Existing generalizable models still do not achieve a satisfactory balance between both "generality" and "specialization", as most of them [53, 49] do not fit diverse scenes well out of box, and some [58, 69] will need extra per-scene optimization step.

To fill the aforementioned gap, we propose to introduce and customize the powerful Mixture-of-Experts (MoE) idea [47] into GNT framework, which is composed of a *view transformer* that aggregates multi-view image features and a *ray transformer* that decodes the point feature to synthesize novel views. The inspiration is drawn from *Large Language Models* (**LLMs**) [27, 12], where MoE has become

---

*Equal contribution.

1

the key knob to improve the generalization of these models, scaling up the total model size without exploding the per-inference cost, by encouraging different submodels (combination of activated experts) to be sparsely activated for different inputs and hence become "specialized".

Specifically, to balance between cross-scene "generalization" and per-scene "specialization", we bake MoE into GNT's view transformer[1], leading to a new GNT with Mixture-of-View-Experts (**GNT-MOVE**). However, as we observed from experiments, naively plugging MoE into NeRF fails to well balance between generality and specialization, due to their intension with generalizable NeRF's cross-scene **consistency** and spatial **smoothness** priors:

- Cross-scene **consistency**: similar appearance patterns or similar materials, from different scenes, should be treated consistently by choosing similar experts.

- Spatial **smoothness**: nearby views in the same scene should change continuously & smoothly, hereby making similar or smoothly transiting expert selection.

Those two "priors" are owing to the natural image rendering and multi-view geometry constraints. Yet, enforcing them risks causing the notorious representation collapse of MoEs [76], i.e., differently activated submodels may naively learn the same or similar functions and be unable to capture diverse specialized features. Such representational collapse has been addressed a lot in the general MoE literature [77, 28, 44]. But it remains elusive whether those solutions will be at odds with the "consistency/smoothness": *a new challenge we must pay attention to*.

In order to mitigate such gaps, we investigate two customized improvements of MoE for NeRF. Firstly, we augment the MoE layer with a shared permanent expert, that will be selected in all cases. This shared expert enforces the commodity across scenes as an architectural regularization, and boosts cross-scene consistency. Secondly, a spatial smoothness objective is introduced for geometric-aware continuity, by encouraging two spatially close points to choose similar experts, and using the geometric distance between sampled points to re-weight their expert selections. We empirically find the two consistency regularizations to work well with the typical expert diversity regularizer in MoEs, together ensuring effectively large model capacity as well as meeting the consistency/smoothness demands. We have conducted comprehensive experiments on complex scene benchmarks. Remarkably, when trained on multiple scenes, GNT-MOVE attains state-of-the-art performance in two aspects: (1) often notably better zero-shot generalization to unseen scenes; and (2) consistently stronger performance on few-shot generalization to unseen scenes.

---

[1]In this paper, we mainly focus on the view transformer based on the hypothesis that the modular design of MoE could be naturally beneficial to multi-view feature aggregation. Introducing MoE into the ray transformer may be also promising and we leave it as future work.

Our main contributions can be summarized as follows:

- We present an LLM-inspired NeRF framework, GNT-MOVE, which significantly pushes the frontier of generalizable novel view synthesis on complex scenes by introducing Mixture-of-Experts (MoE) transformers.

- To tailor MoE for generalizable NeRF, we introduce a shared permanent expert for cross-scene rendering consistency, and a geometry-aware spatial consistency objective for cross-view spatial smoothness.

- Experiments on complex scene benchmarks validate the effectiveness of GNT-MOVE on cross-scene generalization with both zero-shot and few-shot settings.

2. Related Works

NeRF and Its Generalization. Novel View Synthesis (NVS) aims to generate unseen views given a set of posed images. Recently, Neural Radiance Field (*i.e.*, NeRF [34]) has achieved remarkable performance on novel view synthesis by volume rendering on a radiance field. Several followups extend NeRF by proposing new parameterizations of rays [3, 4] to improve rendering quality, using explicit data structures or distillation [15, 31, 52, 35, 56, 17, 19] to improve efficiency, or adopting spatial-temporal modeling [37, 40, 16, 29, 63] to extend it to dynamic scenarios.

However, the original NeRF needs to retrain on each new scene, thus limiting its practical applications. To tackle the cross-scene generalization, one line of works [55, 21, 70] incorporate a convolutional encoder and use the same MLP conditioned on different image features to model different objects. More recently, another line of works [53, 50, 26, 38, 74, 58] adopt transformer-based network with epipolar constraints to synthesize novel views of unseen scenes in a "feedforward" fashion on the fly. Our method is also based on the transformer to render novel scenes in a feedforward fashion. The difference is that we customized the powerful MoE ideas into our framework to balance between cross-scene generalization and per-scene specialization, thus capable of modeling diverse complex scenes and rendering more realistic results, in few- or zero-shot.

Mixture-of-Experts (MoE). MoEs [20, 23, 6, 71, 44, 11, 7] perform input-dependent computations with a combination of sub-models (a.k.a. experts) according to certain learned or ad-hoc routing policies [9, 44]. Various successful cases of MoE have been shown in a wide range of applications. Recent advances [47, 27, 12, 48] in the natural language processing field propose sparse-gated MoEs to scale up LLM capacity without sacrificing per-inference cost and encourage different modules with distinct functionalities. This helps to unleash the massive potential for compositional unseen generalization [68, 32, 67] besides excellent accuracy-efficiency trade-offs. MoE also gains
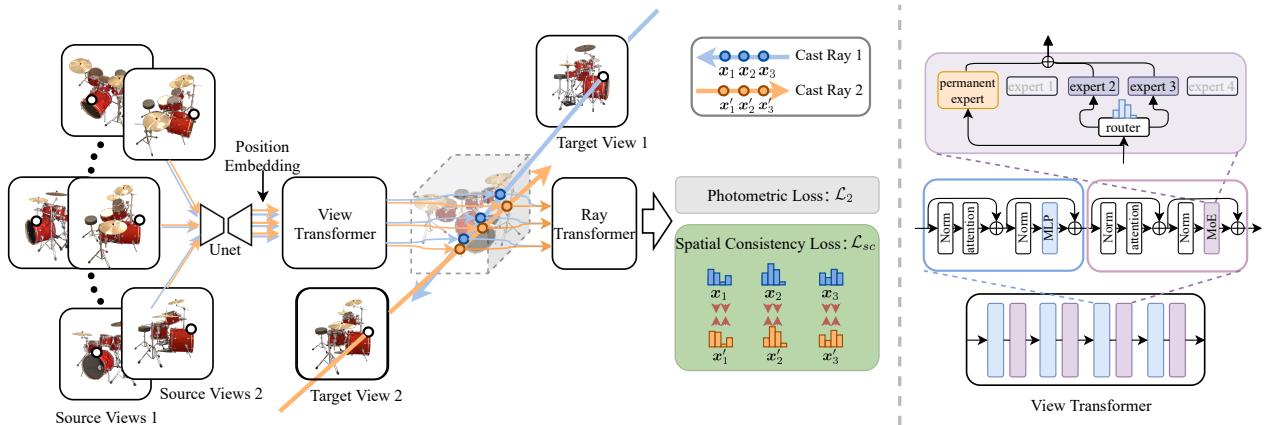
Figure 1: **Overview of our GNT-MOVE.** *Left sub-figure*: for each ray in the target view, sampled points will aggregate multi-view features from source views by passing through the view transformer. *Right sub-figure*: in view transformer, we embed the MoE layer in the transformer blocks. Point token will be processed by both router-selected experts and our proposed permanent expert to enforce cross-scene consistency. Note that we use 4 MoE embedded transformer blocks, and 4 experts per MoE layer, leading to $\binom{4}{2}^4 = 1{,}296$ total expert combinations to provide sufficiently large and diverse coverage.

popularity in computer vision [1, 11, 39], although most works [10, 2, 18, 59, 66] only focus on classification tasks.

A few works have explored the sparsely activated sub-models idea implicitly in NeRF. Kilo-NeRF [41] introduces thousands of tiny MLPs to divide and conquer the entire scene modeling. Block-NeRF [54] enables NeRF to represent a street-scale scene by dividing large environments into individually trained NeRFs. NID [57] improves both data and training efficiency of INR by assembling a group of coordinate-based sub-networks. NeurMiPs [30] leverages a collection of local planar experts in 3D space to boost the reconstruction quality. Different from all previous arts trying to improve per-scene rendering or fitting, we make the first attempt to customize MoE for generalizable NeRF and improve its performance on rendering novel unseen scenes.

3. Preliminary

GNT Generalizable NeRF Transformer (GNT) [53] is a pure, unified transformer-based architecture that efficiently reconstructs Neural Radiance Fields (NeRFs) on the fly from source views. It is composed of two transformer-based stages. In the first stage, the *view transformer* predicts coordinate-aligned features for each point by aggregating information from epipolar lines of its neighboring views. In the second stage, the *ray transformer* composes point-wise features along the ray to compute the ray color. More precisely, given N source images $\{\mathbf{I}_i \in \mathbb{R}^{H \times W \times 3}\}_{i=1}^{N}$, for each sampled point $\boldsymbol{x} \in \mathbb{R}^3$ on a ray emitted from the target view, the view transformer is formulated as:

$$\mathcal{F}(\boldsymbol{x}, \boldsymbol{\theta}) = \text{V-Trans}(\mathbf{F}(\Pi_1(\boldsymbol{x})), ..., \mathbf{F}(\Pi_N(\boldsymbol{x}))), \quad (1)$$

where $\Pi_i(\boldsymbol{x})$ is to project 3D point $\boldsymbol{x}$ onto the i-th image plane $\mathbf{I}_i$, and $\mathbf{F}$ is a small U-Net [45] based CNN that interpolates features at the projected image point. The view transformer is adopted to combine all the extracted features into a coordinate-aligned feature volume.

These multi-view aggregated features are then fed into the ray transformer. The ray transformer then performs mean pooling over the predicted tokens and map them to RGB via an MLP to obtain the rendered ray color:

$$\mathcal{C}(r) = \text{MLP} \circ \text{R-Trans}(\mathcal{F}(\boldsymbol{x}_1, \boldsymbol{\theta}), ..., \mathcal{F}(\boldsymbol{x}_M, \boldsymbol{\theta})). \quad (2)$$

$\{\boldsymbol{x}_1, ..., \boldsymbol{x}_M\}$ are 3D points sampled along the same ray r. In this work, we choose GNT as the backbone due to its outstanding performance. However, our methodology shall be general to other transformer-based NeRFs [50, 26, 38]

MoE A Mixture of Experts (MoE) layer typically contains a group of E experts $f_1, f_2, \cdots, f_E$ and a router $\mathcal{R}$ whose output is an E-dimensional vector. The expert networks are in the form of a multi-layer perception [12, 43] in ViTs. The router $\mathcal{R}$ plays the role of expert selection, and we adopt a representative router called top-K gating [47]. With input token $\mathbf{x}$, the resultant output $\mathbf{y}$ of MoE layers can be formulated as the summation of the selected top K experts from E expert candidates using a router:

$$\mathbf{y} = \sum_{e=1}^{E} \mathcal{R}(\mathbf{x})_e \cdot f_e(\mathbf{x}),$$

$$\mathcal{R}(\mathbf{x}) = \text{softmax}(\text{TopK}(\mathcal{G}(\mathbf{x}), K)),$$

$$\text{TopK}(\mathbf{v}, K)_i = \begin{cases} v_i & \text{if } v_i \text{ is in the top } K \text{ elements of } \mathbf{v} \\ 0 & \text{otherwise} \end{cases}$$

$$(3)$$

where $\mathcal{G}$ represents the learnable network within the router.

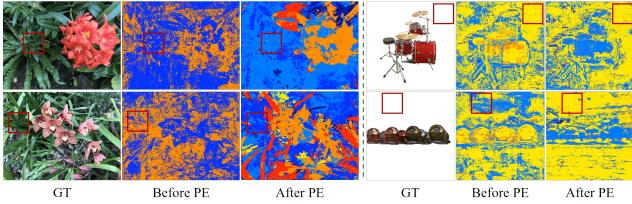GT | Before PE | After PE | GT | Before PE | After PE

Figure 2: **Cross-scene inconsistency.** For similar colors or patterns from different scenes (left: green leaves in Flower and Orchids, right: white background in Drums and Materials), the router selects different experts (visualized with different colors). A permanent expert enforces commodity across scenes to enhance cross-scene consistency.

4. Method

Overview. We scale up GNT model with MoE layer in this section. The main pipeline is illustrated in Figure 1. Our design principle is that we only make necessary and minimal modifications to the vanilla GNT to preserve its standardized architecture and ease of use.

4.1. Mixture of View Experts: The Basic Pipeline

It is discussed in [53] that GNT leverages the UNet to extract geometry, appearance, and local light transport information from the 2D images, and view transformer will integrate those features to estimate the point-wise rendering parameters (such as occupancy, transparency, and reflectance) on the latent space for the ray transformer. We notice that the natural shading properties are often exclusive to each other and thus sparsely activated (e.g., diffuse reflection vs. specular reflection). Also in typical rendering engines, displaying a scene usually invokes different graphical shaders to handle spatially varying materials. These observations altogether motivate us to plug MoE modules into the view transformer to specialize different components for specific rendering properties.

Our pipeline could be seen in Figure 1. As shown in the right sub-figure, in the view transformer, we replace the dense MLP layer with a sparsely activated MoE layer composed of a set of half-sized MLP experts $\{f_e\}_{e=1}^E$. As in Equation 3, the output of each MoE layer is the weighted summation of the outputs from the selected top K experts. Considering the view transformer with L MoE-embedded transformer blocks, we note that the number of possible expert combinations can factually reach $\binom{E}{K}^L$, which can provide sufficiently broad and diverse coverage.

Following many MoE prior arts [77, 28, 44], we also enforce balanced and diverse expert usage to avoid representation collapse. Particularly, within each training batch, we sample 3D points x from ray group $\mathbf{R}$, where the rays are emitted from multiple different views of the same scene, and regularize expert selection via Coefficient of Variation

(CV) of the sparse routing [47]:

$$\mathcal{L}_{div} = CV(\underset{r \sim \mathbf{R}}{\mathbb{E}} \underset{\boldsymbol{x} \in r}{\mathbb{E}} \mathcal{R}(\mathbf{x}))$$
$$CV(\boldsymbol{g}) = mean(\boldsymbol{g})/var(\boldsymbol{g}),$$
(4)

where $\mathbf{x}$ is the token embedding of point $\boldsymbol{x}$, and $mean(\cdot)$ and $var(\cdot)$ compute the sample mean and variance of the input vector respectively. The diversity regularizer (4) is a standard idea in MoE. Putting into a NeRF context, it encourages different views to fully exploit the expert space, and different experts to capture nuances of distinct views.

4.2. Fusing Cross-scene Consistency and Spatial Smoothness into MoE

However, our experiments show that naively plugging MoE into NeRF cannot guarantee a good balance between cross-scene generalization and per-scene specialization. This is due the absence of cross-scene consistency and spatial smoothness, which are essential priors for generalizable NeRF. We hence introduce two levels of NeRF-specific customizations for MoE: (i) architecture level: a shared permanent expert responsible for cross-scene consistency, and (ii) objective level: a spatial consistency objective to encode geometric-aware smoothness.

Permanent Shared Expert As aforementioned, for generalizable NeRF trained on complex and diverse scenes, the employed MoE should keep consistent expert selection on similar appearance patterns or similar materials from different scenes. However, this cross-scene consistency for NeRF can be affected by diversified expert usage in MoE. When we directly plug the MoE layers into GNT, we observe an obvious cross-scene inconsistency: as shown in Figure 2. For similar colors or materials from different scenes, the router selects totally different experts (*e.g.*, leaves in the left sub-figure, white background in the right sub-figure), without considering the sensible cross-scene commodity.

Therefore, to enforce said commodity across scenes and improve cross-scene consistency, we propose to modify the MoE layer from an architectural level. This is achieved through the introduction of a shared permanent expert f_p responsible for distilling common knowledge across different scenes. The permanent expert has the same structure as other experts in the MoE. As shown in Figure 1, instead of being selected by the router, it is fixed and participates in the token processing by default. Formally, given an input token $\mathbf{x}$ to the MoE layer, the output $\mathbf{y}$ is computed as:

$$\mathbf{y} = f_p(\mathbf{x}) + \sum_{e=1}^E \mathcal{R}(\mathbf{x})_e \cdot f_e(\mathbf{x})$$
(5)

Geometry-Aware Spatial Consistency Along with the cross-scene consistency, spatial smoothness is another essential characteristic for NeRFs due to the view geometry

4

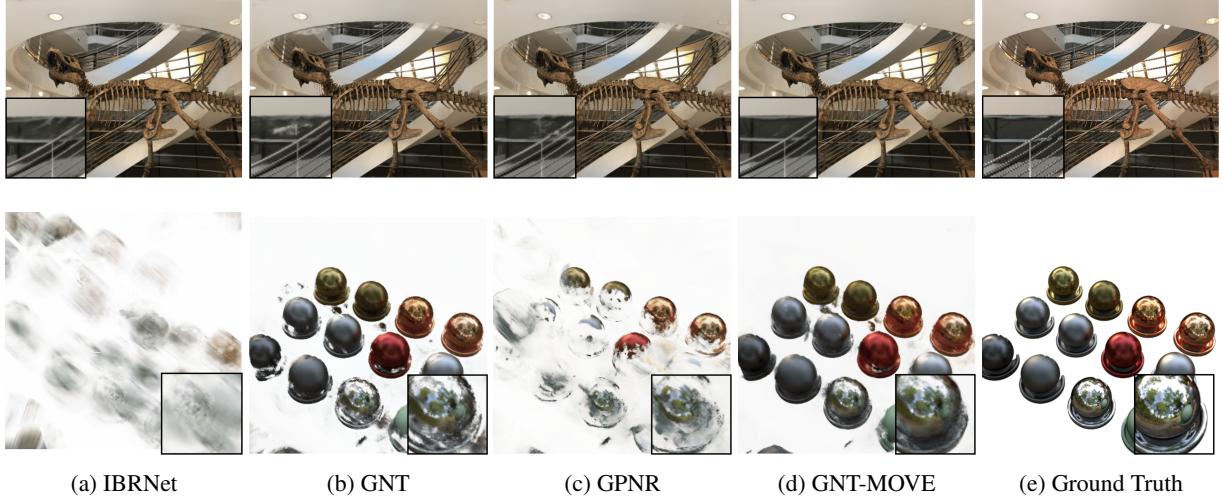| (a) IBRNet | (b) GNT | (c) GPNR | (d) GNT-MOVE | (e) Ground Truth |

Figure 3: Qualitative results for the unseen cross-scene rendering. In the T-Rex scenes (row 1), GNT-MOVE reconstructs the edge details of stairs more accurately. In the Materials scenes (row 2), GNT-MOVE models the complex lighting effects much clearer compared to other methods, showing its stronger generalization ability in modeling different complex scenes.
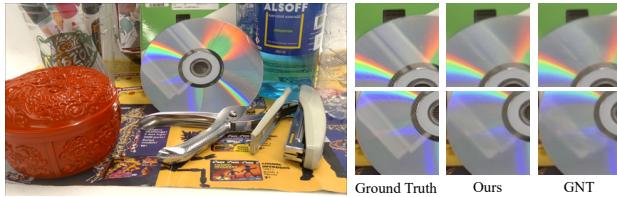

Figure 4: Qualitative comparison on Shiny-6 dataset. From left to right are the ground truth image, and the zoom-in results of GNT-MOVE and GNT, respectively
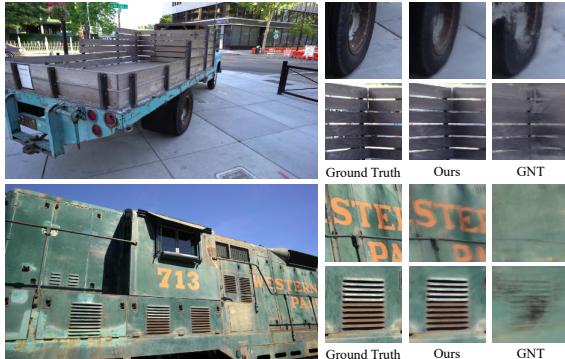

Figure 5: Qualitative comparison on Tanks-and-Temples dataset. From left to right are the ground truth image, and the zoom-in results of GNT-MOVE and GNT, respectively

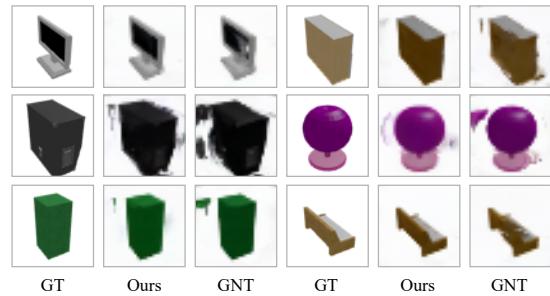| GT | Ours | GNT | GT | Ours | GNT |

Figure 6: Qualitative comparison on NMR dataset. From left to right are the ground truth image, and the zoom-in results of GNT-MOVE and GNT, respectively.

constraints. Seeing from different camera poses, the nearby views in the same scene should make a similar or smoothly transiting expert selection. To encourage such a multi-view consistency, we propose a spatial consistency objective that encourages two spatially close points to choose similar ex-

perts, and we use the geometric distance between them to re-weight the expert selection.

Specifically, given two spatially close 3D points x_i and x_j, the router $\mathcal{R}$ takes their token embedding $\mathbf{x}_i$ and $\mathbf{x}_j$ as input and maps them to expert selection scores $R(\mathbf{x}_i), R(\mathbf{x}_j) \in \mathbb{R}^E$ respectively. Similar expert selection is thereby encouraged through *pulling* these two distributions closer. However, as we have a huge amount of sampled points from multiple views, it is computationally expensive and inefficient to calculate the pairwise distance between all 3D points. To make it easier to find pairs of close points, we first calculate the pairwise distance between rays based on their location in the image coordinate system. Then we filter out close rays whose pairwise distance is smaller than a predefined threshold ϵ. For 3D points sampled from two close rays, we compute the Euclidean distance between all the points, denoted as $d_{i,j} = \|x_i - x_j\|$. For each point x_i, we select its closest points x_i' with dis-

tance $d_{i,i'}$. Therefore, we encourage the consistency of the expert selection between the closest points via a symmetric Kullback–Leibler divergence loss:

$$\mathcal{L}_{KL}(\boldsymbol{x}_i) = \frac{1}{2} D_{KL}(R(\mathbf{x}_i)\|R(\mathbf{x}_i')) + \frac{1}{2} D_{KL}(R(\mathbf{x}_i')\|R(\mathbf{x}_i)). \quad (6)$$

As closer points are more likely to have higher expert selection similarity, we do not treat all pairs equally. Rather we use their geometric distances to serve as a consistency confidence $\rho_i = \frac{e^{-d_{i,i'}}}{\sum_{(\boldsymbol{x}_j,\boldsymbol{x}_j')} e^{-d_{j,j'}}}$. The final spatial consistency loss is hence defined as:

$$\mathcal{L}_{\text{sc}} = \sum_{(\boldsymbol{x}_i,\boldsymbol{x}_i')} \rho_i \mathcal{L}_{KL}(\boldsymbol{x}_i). \quad (7)$$

Note that our spatial consistency is enforced on 3D points from multiple views. Therefore, it naturally encourages geometry-aware spatial smoothness in the same scene.

5. Experiments

In this section, we conduct extensive experiments with GNT-MOVE to answer two questions: *i) Does MoE help GNT scale up in scene coverage and improve generality? ii) Does GNT-MOVE meanwhile improve specialization to different scenes?* We compare GNT-MOVE with state-of-the-art (SOTA) methods on generalizable novel view synthesis tasks, under both zero-shot and few-shot settings (Section 5.2). We also provide careful analyses on the expert selection in GNT-MOVE to illustrate how MoE divide and conquer to render a challenging scene (Section 5.4).

5.1. Implementation Details

Training / Inference Details We choose top $K = 2$ experts out of $E = 4$ expert candidates per layer. Note that we scale down the expert size by half compared to the dense MLP layer in standard ViT to make their computation FLOPs equivalent. We train GNT-MOVE end-to-end using the Adam optimizer. The threshold ϵ for close rays is set as 20. The loss weights λ_{sc} and λ_{div} are set to be 1×10^4 and 1×10^{-3}, respectively. Please refer to our supplementary for additional training details.

Metrics We adopt three widely-used metrics: Peak Signal-to-Noise Ratio (PSNR), Structural Similarity Index Measure (SSIM) [60], and the Learned Perceptual Image Patch Similarity (LPIPS) [73]. We report the average of each metric across multiple scenes in one dataset for cross-scene generalization experiments. Following [53], we also report the geometric mean of $10^{-PSNR/10}, \sqrt{1 - SSIM}$, LPIPS, for an easier comparison [3].

5.2. Main Experiments: Zero-Shot and Few-Shot Cross-Scene Generalization

Setting To evaluate the cross-scene generalization performance, we compare our GNT-MOVE with state-of-the-art generalizable NeRF under two important settings:

- **Zero-shot**: the pre-trained model is directly evaluated on an unseen scene for novel view synthesis.

- **Few-shot**: the pre-trained model is first finetuned with a few observed views from the target unseen scene, and then applied to the target scene.

Datasets We follow the experimental protocol in IBR-Net [58] and GNT [53] and use the following training/evaluation datasets: (1) **Training Datasets** consist of both real and synthetic data, in consistency with GNT [53]. For synthetic data, we use object renderings of 1023 models from Google Scanned Object [8]. For real data, we make use of RealEstate10K [75], 90 scenes from the Spaces dataset [13], and 102 real scenes from handheld cellphone captures [33, 58]. (2) **Testing Datasets** are the common NeRF benchmarks including Local Light Field Fusion (LLFF) [33] and NeRF Synthetic dataset [34]. Note that these LLFF scenes are not included in the handheld cellphone captures in the training set. We also include *three additional datasets*: Shiny-6 dataset [62], Tanks-and-Temples [42] and NMR [24], which contains complex optical effects, large unbounded scenes, and 360° views of various objects from unseen categories, respectively. More dataset details can be found in the supplementary.

5.2.1 Zero-Shot Generalization

For LLFF and NeRF Synthetic scenes, we compare our method with PixelNeRF [70], MVSNeRF [5], IBRNet [58], GNT [53], and GPNR [49]. As seen from Table 1a, our method achieves the best performance on both LLFF and NeRF Synthetic datasets in PSNR, LPIPS, and average evaluation metrics. Compared with GPNR, GNT-MOVE achieves a significantly better perceptual score, with up to 38% LPIPS reduction on both datasets. We also outperform GNT on PSNR with notable improvements of 0.16dB and 0.18dB on two datasets. The qualitative results on representative scenes are shown in Figure 3. One could observe that GNT-MOVE renders novel views with clearly better visual quality. It particularly better reconstructs fine details of object edges in T-Rex, and more accurately models complex specular reflection effects in Materials (even our training sets contain only limited lighting variations).

We then compare on the more challenging Shiny [62], Tanks-and-Temples [42], and NMR [24] datasets. On the non-object-centric Shiny dataset, we observe from Table 1b that, GNT-MOVE clearly surpasses its peers of the generalizable category in all the metrics: outperforming GNT

Models	Local Light Field Fusion (LLFF)				NeRF Synthetic			
	PSNR↑	SSIM↑	LPIPS↓	Avg↓	PSNR↑	SSIM↑	LPIPS↓	Avg↓
PixelNeRF	18.66	0.588	0.463	0.159	22.65	0.808	0.202	0.078
MVSNeRF	21.18	0.691	0.301	0.108	25.15	0.853	0.159	0.057
IBRNet	25.17	0.813	0.200	0.064	26.73	0.908	0.101	0.040
GPNR	25.72	**0.880**	0.175	0.055	26.48	**0.944**	0.091	0.036
GNT	25.86	0.867	0.116	0.047	27.29	0.937	0.056	0.029
Ours	**26.02**	0.869	**0.108**	**0.043**	**27.47**	0.940	**0.056**	**0.029**

(a) NeRF Synthetic dataset and LLFF dataset.

Setting	Models	Shiny-6 Dataset			
		PSNR↑	SSIM↑	LPIPS↓	Avg↓
Per-Scene Training	NeRF	25.60	0.851	0.259	0.065
	NeX	26.45	0.890	0.165	0.049
	IBRNet	26.50	0.863	0.122	0.047
	NLF	27.34	0.907	0.045	0.029
Generalizable	IBRNet	23.60	0.785	0.180	0.071
	GPNR	24.12	0.860	0.170	0.063
	GNT	27.10	0.912	0.083	0.036
	Ours	**27.54**	**0.932**	0.072	0.032

(b) Shiny dataset.

Models	NMR Dataset			
	PSNR ↑	SSIM ↑	LPIPS ↓	Avg ↓
LFN	24.95	0.870	-	-
PixelNeRF	26.80	0.910	0108	0.041
SRT	27.87	0.912	0.066	0.032
GNT	32.12	0.970	0.032	0.015
Ours	**33.08**	**0.972**	**0.031**	**0.014**

(c) NMR dataset.

Setting	Models	Truck			Train			M60			Playground		
		PSNR↑	SSIM↑	LPIPS↓	PSNR↑	SSIM↑	LPIPS↓	PSNR↑	SSIM↑	LPIPS↓	PSNR↑	SSIM↑	LPIPS↓
Per-scene Training	NeRF	20.85	0.747	0.513	16.64	0.635	0.651	16.86	0.702	0.602	21.55	0.765	0.529
	NeRF++	22.77	0.823	0.298	17.17	0.672	0.523	17.88	0.738	0.435	22.37	0.799	0.391
Generalizable	GNT	17.39	0.561	0.429	14.09	0.420	0.552	11.29	0.419	0.605	15.36	0.417	0.558
	Ours	19.71	0.628	0.379	16.27	0.499	0.466	13.56	0.495	0.527	19.10	0.501	0.507

(d) Tanks-and-Temples dataset.

Table 1: Comparison of GNT-MOVE against SOTA methods for cross-scene generalization under **zero-shot setting**.

Models	Local Light Field Fusion (LLFF)												NeRF Synthetic							
	3-shot				6-shot				10-shot				6-shot				12-shot			
	PSNR↑	SSIM↑	LPIPS↓	Avg↓	PSNR↑	SSIM↑	LPIPS↓	Avg↓	PSNR↑	SSIM↑	LPIPS↓	Avg↓	PSNR↑	SSIM↑	LPIPS↓	Avg↓	PSNR↑	SSIM↑	LPIPS↓	Avg↓
PixelNeRF	17.54	0.543	0.502	0.181	19.00	0.721	0.496	0.148	20.01	0.755	0.333	0.123	19.13	0.783	0.250	0.112	21.90	0.849	0.173	0.075
MVSNeRF	17.05	0.486	0.480	0.189	20.50	0.594	0.384	0.130	22.54	0.673	0.309	0.099	16.74	0.781	0.263	0.138	22.06	0.844	0.185	0.076
IBRNet	16.89	0.539	0.458	0.185	20.61	0.686	0.316	0.115	23.52	0.789	0.226	0.077	18.17	0.812	0.234	0.115	24.69	0.895	0.120	0.051
GNT	19.58	0.653	0.279	0.121	22.36	0.766	0.189	0.081	24.14	0.834	0.133	0.059	22.39	0.856	0.139	0.067	25.25	0.901	0.088	0.044
Ours	**19.71**	**0.666**	**0.270**	**0.120**	**22.53**	**0.774**	**0.184**	**0.078**	**24.61**	**0.837**	**0.132**	**0.056**	**22.53**	**0.871**	**0.116**	**0.061**	**25.85**	**0.915**	**0.074**	**0.038**

Table 2: Comparison of GNT-MOVE against SOTA methods in **few-shot setting** on the LLFF and NeRF Synthetic datasets.

by 0.44 dB PSNR, and GPNR/IBRNet by over 3 dB. Even compared to the per-scene fitting category (which puts an unfair disadvantage on us), our PSNR and SSIM still win over strong competitors such as NLF (which has particular optical modeling) and IBRNet. All those results endorse that GNT-MOVE benefits its MoE-based specialization to adapt well to challenging materials and light effects.

We further compare GNT-MOVE with SRT [46], another transformer-based renderer pre-trained by novel view synthesis, on the NMR dataset [24]. As shown in Table 1c, GNT-MOVE remarkably outperforms SRT by 5.21 dB PSNR - that is even more impressive if one considers that SRT is pre-trained with samples from NMR. In contrast, GNT-MOVE can "zero-shot" generalize way better. It also outperforms GNT by a remarkable 1 dB PSNR. Table 1d also demonstrates the performance of GNT-MOVE on the Tanks-and-Temples dataset (the four scenes selected in NeRF++[72]). Once again, GNT-MOVE largely outperforms GNT by up to 3 dB PSNR. Those results strongly suggest that GNT-MOVE, with its higher capacity, is indeed more generalizable and robust than vanilla GNT. The qualitative rendering comparison on representative scenes from Shiny-6 dataset [62], Tanks-and-Temples dataset [42], and NMR dataset [24] could be found in Figure 4, Figure 5, and Figure 6, respectively.

5.2.2 Few-Shot Generalization

Next under the few-shot setting, we compare our method with PixelNeRF [70], MVSNeRF [5], IBRNet [58], and GNT [53]. On the LLFF dataset that contains forward-facing scenes, we finetune the pre-trained models using 3, 6, and 10 images. On NeRF Synthetic dataset that contains 360° scenes, we finetune them on 6 and 12 images, respectively. During inference, images used for finetuning are by default included as source images for novel view synthesis.

In Table 2, GNT-MOVE shows a remarkably large performance gain over all the state-of-the-art methods on NeRF Synthetic dataset. Compared to GNT, our model achieves better results in all metrics, with particularly impressive perceptual score gains of 17% and 16% LPIPS on 6-shot and 12-shot, respectively. GNT-MOVE also improves over GNT by a great margin of 0.6 dB PSNR and 0.14 SSIM on 12-shot setting. Similar performance gains are also observed on the LLFF dataset: GNT-MOVE improves the state-of-the-art GNT on PSNR metric by 0.13 dB, 0.17 dB, and 0.47 dB on 3-shot, 6-shot, and 10-shot, respectively.

5.3. Spotlight Comparison: GNT v.s. GNT-MOVE

Since GNT-MOVE is an extension of GNT (which is the most recent SOTA), it is naturally of interest to compare the two closely and to understand how much benefits MoE actually brings to GNT ("specialization" v.s. "generalization"), for the goal of cross-scene generalization. While most aforementioned experiments already demonstrate various solid gains, we feel it worthy of providing a focused summary below. We emphasize that GNT and GNT-MOVE are trained and evaluated in completely fair settings.
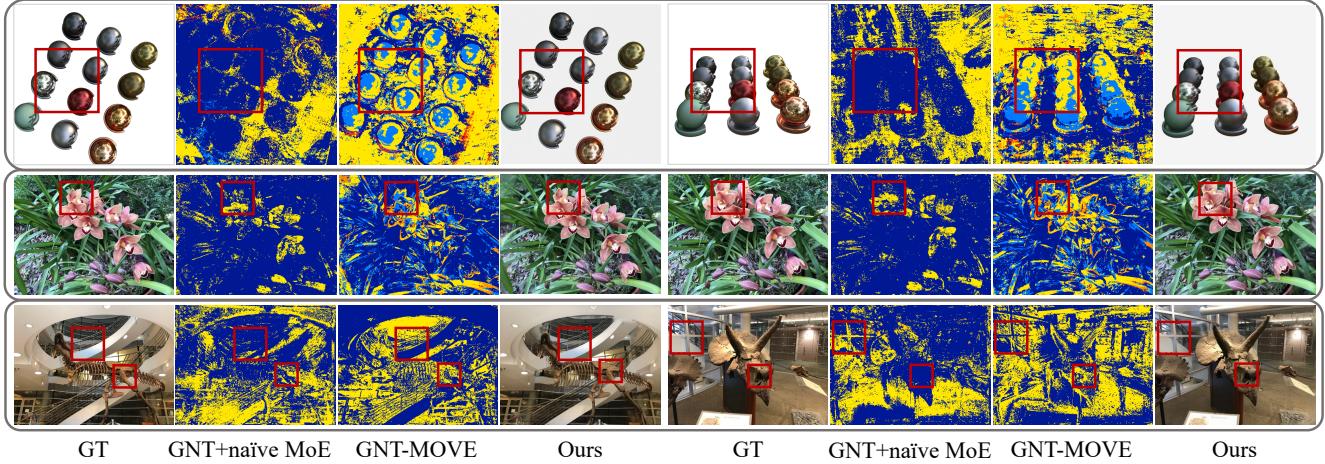
- In the zero-shot setting, GNT-MOVE always outper-

Figure 7: Visualization of expert selection using different colors. Row 1: two quite different views from the Materials scene. Row 2: two slightly different views from the Orchids scene. Row 3: two different scenes, but with similar visual appearances (*e.g.*, stairs, bones). We compare GNT with naive MoE, and our GNT-MOVE solution.

forms GNT on the metric of PSNR, with moderate improvements of **0.16 dB** and **0.18 dB**, on the "standard" LLFF and NeRF Synthetic datasets, respectively. Yet on the more challenging ones, the PSNR gain of GNT-MOVE over GNT becomes larger: **0.44 dB** on Shiny, **0.96 dB** on NMR, and eventually an impressive **2.63 dB** on Tanks-and-Temples (averaged over 4 scenes).

- Same in the zero-shot setting, GNT-MOVE outperforms GNT in all cases on the metrics of LPIPS and Avg scores. It marginally lags behind GPNR on SSIM in NeRF Synthetic and LLFF, but wins on SSIM on other more challenging datasets. For example, the SSIM gain of GNT-MOVE over GNT is as large as 0.076 on Tanks-and-Temples (averaged over 4 scenes).

- Then, in the few-shot setting, our results suggest a **clean sweep** for GNT-MOVE, in all shot settings, under all metrics, on both LLFF and NeRF Synthetic datasets. Generally, as the number of shots increases, the gains of GNT-MOVE over GNT seem to increase as well, ending up with **0.47 dB** and **0.60 dB** gaps on LLFF and NeRF synthetic, respectively.

- When it comes to visual quality, GNT-MOVE is clearly superior in tackling challenging scenes with complex lighting, e.g., Ship, Materials, and Drums (please refer to the per-scene breakdown results of zero-shot generalization in the supplementary). The experiments on the Shiny dataset in Table 1b demonstrate that GNT-MOVE generalizes better than GNT in the presence of challenging refraction and reflection.

- Also in Table 1d, GNT-MOVE generalizes out of the box on large-scale, unbounded 3D scenes while the vanilla GNT fails. Note that both GNT-MOVE and
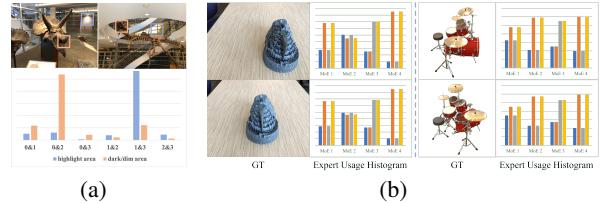

Figure 8: Expert selection histogram. (a) Similar patterns (e.g., bright) across different scenes have similar expert selections; (b) Different views from the same scene have similar and consistent layer-wise expert selections.

GNT are trained only on bounded and forward-facing scenes, implying the stronger compositional generalization potential [25] achieved through MoEs.

More comparisons, demonstrating that the solid gain of MoE for generalizable NeRF goes way beyond naively larger model size; yet the gain can only be unleashed with PE and SR, could be found in the supplementary.

5.4. Dive into the Expert Selection

GNT-MOVE strikes a good balance between cross-scene/view consistency and expert specialization: it can be demonstrated through the visualization of expert maps in Figure 7, where we compare GNT-MOVE with a baseline of GNT + naive MoE (i.e., the basic pipeline described in Sec. 4.1, without enforcing our customized consistency/smoothness).

In Row 1, two different views of the Materials scene select the same set of experts for foreground material balls and the background, respectively. That is in contrast to the much more confused/"mixed" selection observed in GNT + naive MoE. In Row 2, one observes the same cross-view consistency, while the subtle differences between two views

8

Models				Local Light Field Fusion (LLFF)				NeRF Synthetic			
	MoE	PE	SR	PSNR↑	SSIM↑	LPIPS↓	Avg↓	PSNR↑	SSIM↑	LPIPS↓	Avg↓
GNT	–	–	–	25.86	0.867	0.116	0.047	27.29	0.937	0.056	0.029
Ours	✓			25.46	0.856	0.128	0.051	27.15	0.934	0.057	0.031
Ours	✓	✓		25.88	0.865	0.120	0.049	27.32	0.936	0.058	0.030
Ours	✓		✓	25.93	0.866	0.117	0.046	27.30	0.935	0.059	0.030
Ours	✓	✓	✓	**26.02**	**0.869**	**0.108**	**0.043**	**27.47**	**0.940**	**0.056**	**0.029**

Table 3: Ablation analyses of our two key proposals: PE indicates permanent expert and SR indicates smoothness regularizer.

(*e.g.*, occluded bud) are also modeled differently in the two corresponding expert maps, indicating good expert specialization and diversity. Row 3 indicates an example of cross-scene consistency, where the same expert group is selected by GNT-MOVE for similar visual appearances (*e.g.*, stairs, bones) across two different scenes.

The selection of experts also properly reacts to fine edges (*e.g.*, flower edges in row 2, handrail edge and bone edge in row 3), and is also capable of adapting to complex lighting effects, as shown in the Materials scene (row 1) and the light part of the T-Rex scene (row 3 right). Furthermore, we visualize the expert selection histogram in Figure 8. It aligns well with our observations that GNT-MOVE excels in ensuring both cross-scene consistency and cross-view spatial smoothness. In Figure 8a, by aggregating expert selections from all test frames of the {Trex, Horns} scenes, we discern that experts 1&3 are predominantly chosen for bright patterns, whereas experts 0&2 are favored for darker or dimmer regions. Concurrently, Figure 8b underscores that expert selections across varied views of the same scene exhibit layer-wise similarity and consistency.

Besides, following [53], we plot the depth maps computed from the learned attention values in Figure 9. The depth maps show clear physical ground that GNT-MOVE learns the correct geometry without explicit supervision. It also confirms that our geometry-aware smoothness does not distort or oversmooth the geometry.

5.5. Ablation Studies

We conduct ablation analysis on our key proposals, permanent expert and smoothness regularizer, on cross-scene generalization under zero-shot setting, and report results on the LLFF [33] and NeRF Synthetic dataset [34] in Table 3.

As observed, directly plugging MoE into GNT cannot guarantee a good performance. We witness a performance drop on both datasets after adding the MoE. This is because MoE does not meet NeRF's cross-view consistency requirements and also does not learn the commodity across different scenes. Evidently, our customized design of permanent expert and smoothness regularizer both aid in improving model generalization capability. On the LLFF dataset, the smoothness regularizer brings the biggest per-
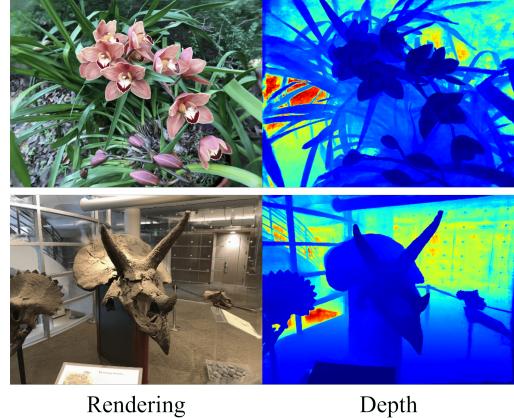

Rendering   Depth

Figure 9: Geometry visualization. We show the depth maps from GNT-MOVE. Red indicates far and blue is near.

formance gain, as cross-view consistency naturally benefits scenes with slightly disturbed views. On the NeRF Synthetic dataset with diverse complex scenes and materials, the permanent expert brings a considerable improvement as it enforces the commodity across scenes, thus contributing to the cross-scene consistency. Qualitative results in Figure 7 also illustrate their gains over the naive plug-in of MoE.

6. Conclusion

In this work, we focus on generalizable novel view synthesis on complex scenes and propose a novel learning-based framework, GNT-MOVE, that significantly pushes the frontier of this problem by introducing MoE to the domain of NeRFs. In order to better tailor MoE for generalizable NeRFs, we introduce a shared permanent expert and a spatial consistency objective to enforce cross-scene consistency and geometry-aware smoothness. GNT-MOVE proves its effectiveness by achieving SOTA performance on cross-scene generalization in both zero-shot and few-shot settings, on a broad collection of datasets. Our limitation is that we primarily focus on the view transformer of GNT, while introducing MoE into the ray transformer may be further promising - we regard it as future work.

References

[1] Alhabib Abbas and Yiannis Andreopoulos. Biased mixtures of experts: Enabling computer vision inference under data transfer limitations. *IEEE Transactions on Image Processing*, 29:7656–7667, 2020. 3

[2] Karim Ahmed, Mohammad Haris Baig, and Lorenzo Torresani. Network of experts for large-scale image categorization. In *European Conference on Computer Vision*, pages 516–532. Springer, 2016. 3

[3] Jonathan T Barron, Ben Mildenhall, Matthew Tancik, Peter Hedman, Ricardo Martin-Brualla, and Pratul P Srinivasan. Mip-nerf: A multiscale representation for anti-aliasing neural radiance fields. In *Proceedings of the IEEE/CVF International Conference on Computer Vision*, pages 5855–5864, 2021. 1, 2, 6

[4] Jonathan T Barron, Ben Mildenhall, Dor Verbin, Pratul P Srinivasan, and Peter Hedman. Mip-nerf 360: Unbounded anti-aliased neural radiance fields. In *Proceedings of the IEEE/CVF Conference on Computer Vision and Pattern Recognition*, pages 5470–5479, 2022. 2

[5] Anpei Chen, Zexiang Xu, Fuqiang Zhao, Xiaoshuai Zhang, Fanbo Xiang, Jingyi Yu, and Hao Su. Mvsnerf: Fast generalizable radiance field reconstruction from multi-view stereo. In *Proceedings of the IEEE/CVF International Conference on Computer Vision*, pages 14124–14133, 2021. 6, 7

[6] Ke Chen, Lei Xu, and Huisheng Chi. Improved learning algorithms for mixture of experts in multiclass classification. *Neural networks*, 12(9):1229–1252, 1999. 2

[7] Tianlong Chen, Zhenyu Zhang, AJAY KUMAR JAISWAL, Shiwei Liu, and Zhangyang Wang. Sparse moe as the new dropout: Scaling dense and self-slimmable transformers. In *The Eleventh International Conference on Learning Representations*, 2023. 2

[8] Laura Downs, Anthony Francis, Nate Koenig, Brandon Kinman, Ryan Hickman, Krista Reymann, Thomas B McHugh, and Vincent Vanhoucke. Google scanned objects: A high-quality dataset of 3d scanned household items. *arXiv preprint arXiv:2204.11918*, 2022. 6

[9] Dheeru Dua, Shruti Bhosale, Vedanuj Goswami, James Cross, Mike Lewis, and Angela Fan. Tricks for training sparse translation models. *arXiv preprint arXiv:2110.08246*, 2021. 2

[10] David Eigen, Marc'Aurelio Ranzato, and Ilya Sutskever. Learning factored representations in a deep mixture of experts. *arXiv preprint arXiv:1312.4314*, 2013. 3

[11] Zhiwen Fan, Rishov Sarkar, Ziyu Jiang, Tianlong Chen, Kai Zou, Yu Cheng, Cong Hao, Zhangyang Wang, et al. M³vit: Mixture-of-experts vision transformer for efficient multi-task learning with model-accelerator co-design. *Advances in Neural Information Processing Systems*, 35:28441–28457, 2022. 2, 3

[12] William Fedus, Barret Zoph, and Noam Shazeer. Switch transformers: Scaling to trillion parameter models with simple and efficient sparsity. *arXiv preprint arXiv:2101.03961*, 2021. 1, 2, 3

[13] John Flynn, Michael Broxton, Paul Debevec, Matthew Du-Vall, Graham Fyffe, Ryan Overbeck, Noah Snavely, and Richard Tucker. Deepview: View synthesis with learned gradient descent. In *Proceedings of the IEEE/CVF Conference on Computer Vision and Pattern Recognition*, pages 2367–2376, 2019. 6

[14] Sara Fridovich-Keil, Alex Yu, Matthew Tancik, Qinhong Chen, Benjamin Recht, and Angjoo Kanazawa. Plenoxels: Radiance fields without neural networks. In *Proceedings of the IEEE/CVF Conference on Computer Vision and Pattern Recognition*, pages 5501–5510, 2022. 1

[15] Sara Fridovich-Keil, Alex Yu, Matthew Tancik, Qinhong Chen, Benjamin Recht, and Angjoo Kanazawa. Plenoxels: Radiance Fields Without Neural Networks. In *Proceedings of the IEEE/CVF Conference on Computer Vision and Pattern Recognition*, pages 5501–5510, 2022. 2

[16] Guy Gafni, Justus Thies, Michael Zollhofer, and Matthias Nießner. Dynamic Neural Radiance Fields for Monocular 4D Facial Avatar Reconstruction. In *Proceedings of the IEEE/CVF Conference on Computer Vision and Pattern Recognition*, pages 8649–8658, 2021. 2

[17] Stephan J Garbin, Marek Kowalski, Matthew Johnson, Jamie Shotton, and Julien Valentin. Fastnerf: High-Fidelity Neural Rendering at 200fps. *arXiv preprint arXiv:2103.10380*, 2021. 2

[18] Sam Gross, Marc'Aurelio Ranzato, and Arthur Szlam. Hard mixtures of experts for large scale weakly supervised vision. In *Proceedings of the IEEE Conference on Computer Vision and Pattern Recognition*, pages 6865–6873, 2017. 3

[19] Peter Hedman, Pratul P Srinivasan, Ben Mildenhall, Jonathan T Barron, and Paul Debevec. Baking Neural Radiance Fields for Real-Time View Synthesis. *arXiv preprint arXiv:2103.14645*, 2021. 2

[20] Robert A Jacobs, Michael I Jordan, Steven J Nowlan, and Geoffrey E Hinton. Adaptive mixtures of local experts. *Neural computation*, 3(1):79–87, 1991. 2

[21] Wonbong Jang and Lourdes Agapito. Codenerf: Disentangled neural radiance fields for object categories. In *Proceedings of the IEEE/CVF International Conference on Computer Vision*, pages 12949–12958, 2021. 2

[22] Yifan Jiang, Peter Hedman, Ben Mildenhall, Dejia Xu, Jonathan T Barron, Zhangyang Wang, and Tianfan Xue. Alignerf: High-fidelity neural radiance fields via alignment-aware training. In *Proceedings of the IEEE/CVF Conference on Computer Vision and Pattern Recognition*, pages 46–55, 2023. 1

[23] Michael I Jordan and Robert A Jacobs. Hierarchical mixtures of experts and the em algorithm. *Neural computation*, 6(2):181–214, 1994. 2

[24] Hiroharu Kato, Yoshitaka Ushiku, and Tatsuya Harada. Neural 3d mesh renderer. In *Proceedings of the IEEE conference on computer vision and pattern recognition*, pages 3907–3916, 2018. 6, 7, 13

[25] Daniel Keysers, Nathanael Schärli, Nathan Scales, Hylke Buisman, Daniel Furrer, Sergii Kashubin, Nikola Momchev, Danila Sinopalnikov, Lukasz Stafiniak, Tibor Tihon, et al. Measuring compositional generalization: A comprehensive method on realistic data. In *International Conference on Learning Representations*, 2020. 8

[26] Jonáš Kulhánek, Erik Derner, Torsten Sattler, and Robert Babuška. Viewformer: Nerf-free neural rendering from few images using transformers. *arXiv preprint arXiv:2203.10157*, 2022. 2, 3

[27] Dmitry Lepikhin, HyoukJoong Lee, Yuanzhong Xu, Dehao Chen, Orhan Firat, Yanping Huang, Maxim Krikun, Noam Shazeer, and Zhifeng Chen. Gshard: Scaling giant models with conditional computation and automatic sharding. *arXiv preprint arXiv:2006.16668*, 2020. 1, 2

[28] Mike Lewis, Shruti Bhosale, Tim Dettmers, Naman Goyal, and Luke Zettlemoyer. Base layers: Simplifying training of large, sparse models. In *International Conference on Machine Learning*, pages 6265–6274. PMLR, 2021. 2, 4

[29] Tianye Li, Mira Slavcheva, Michael Zollhoefer, Simon Green, Christoph Lassner, Changil Kim, Tanner Schmidt, Steven Lovegrove, Michael Goesele, and Zhaoyang Lv. Neural 3D Video Synthesis. *arXiv preprint arXiv:2103.02597*, 2021. 2

[30] Zhi-Hao Lin, Wei-Chiu Ma, Hao-Yu Hsu, Yu-Chiang Frank Wang, and Shenlong Wang. Neurmips: Neural mixture of planar experts for view synthesis. In *Proceedings of the IEEE/CVF Conference on Computer Vision and Pattern Recognition*, pages 15702–15712, 2022. 3

[31] Lingjie Liu, Jiatao Gu, Kyaw Zaw Lin, Tat-Seng Chua, and Christian Theobalt. Neural Sparse Voxel Fields. *Advances in Neural Information Processing Systems*, 33:15651–15663, 2020. 1, 2

[32] Songhua Liu, Kai Wang, Xingyi Yang, Jingwen Ye, and Xinchao Wang. Dataset distillation via factorization. In *Advances in Neural Information Processing Systems*, 2022. 2

[33] Ben Mildenhall, Pratul P Srinivasan, Rodrigo Ortiz-Cayon, Nima Khademi Kalantari, Ravi Ramamoorthi, Ren Ng, and Abhishek Kar. Local light field fusion: Practical view synthesis with prescriptive sampling guidelines. *ACM Transactions on Graphics (TOG)*, 38(4):1–14, 2019. 6, 9, 13

[34] Ben Mildenhall, Pratul P. Srinivasan, Matthew Tancik, Jonathan T. Barron, Ravi Ramamoorthi, and Ren Ng. Nerf: Representing scenes as neural radiance fields for view synthesis, 2020. 1, 2, 6, 9, 13

[35] Thomas Müller, Alex Evans, Christoph Schied, and Alexander Keller. Instant Neural Graphics Primitives With a Multiresolution Hash Encoding. *ACM Transactions on Graphics (TOG)*, 41:1 – 15, 2022. 2

[36] Michael Niemeyer, Lars Mescheder, Michael Oechsle, and Andreas Geiger. Differentiable volumetric rendering: Learning implicit 3d representations without 3d supervision. In *Proceedings of the IEEE/CVF Conference on Computer Vision and Pattern Recognition*, pages 3504–3515, 2020. 13

[37] Keunhong Park, Utkarsh Sinha, Jonathan T Barron, Sofien Bouaziz, Dan B Goldman, Steven M Seitz, and Ricardo Martin-Brualla. Nerfies: Deformable neural radiance fields. In *Proceedings of the IEEE/CVF International Conference on Computer Vision*, pages 5865–5874, 2021. 2

[38] Navneet Paul. Transnerf-improving neural radiance fields using transfer learning for efficient scene reconstruction. Master's thesis, University of Twente, 2021. 2, 3

[39] Svetlana Pavlitskaya, Christian Hubschneider, Michael Weber, Ruby Moritz, Fabian Huger, Peter Schlicht, and Marius Zollner. Using mixture of expert models to gain insights into semantic segmentation. In *Proceedings of the IEEE/CVF Conference on Computer Vision and Pattern Recognition Workshops*, pages 342–343, 2020. 3

[40] Albert Pumarola, Enric Corona, Gerard Pons-Moll, and Francesc Moreno-Noguer. D-nerf: Neural radiance fields for dynamic scenes. In *Proceedings of the IEEE/CVF Conference on Computer Vision and Pattern Recognition*, pages 10318–10327, 2021. 2

[41] Christian Reiser, Songyou Peng, Yiyi Liao, and Andreas Geiger. Kilonerf: Speeding up neural radiance fields with thousands of tiny mlps. In *Proceedings of the IEEE/CVF International Conference on Computer Vision*, pages 14335–14345, 2021. 1, 3

[42] Gernot Riegler and Vladlen Koltun. Free view synthesis. In *Computer Vision–ECCV 2020: 16th European Conference, Glasgow, UK, August 23–28, 2020, Proceedings, Part XIX 16*, pages 623–640. Springer, 2020. 6, 7, 13

[43] Carlos Riquelme, Joan Puigcerver, Basil Mustafa, Maxim Neumann, Rodolphe Jenatton, André Susano Pinto, Daniel Keysers, and Neil Houlsby. Scaling vision with sparse mixture of experts. *Advances in Neural Information Processing Systems*, 34:8583–8595, 2021. 3

[44] Stephen Roller, Sainbayar Sukhbaatar, Jason Weston, et al. Hash layers for large sparse models. *Advances in Neural Information Processing Systems*, 34:17555–17566, 2021. 2, 4

[45] Olaf Ronneberger, Philipp Fischer, and Thomas Brox. U-Net: Convolutional networks for biomedical image segmentation. In *MICCAI*, 2015. 3

[46] Mehdi SM Sajjadi, Henning Meyer, Etienne Pot, Urs Bergmann, Klaus Greff, Noha Radwan, Suhani Vora, Mario Lučić, Daniel Duckworth, Alexey Dosovitskiy, et al. Scene representation transformer: Geometry-free novel view synthesis through set-latent scene representations. In *Proceedings of the IEEE/CVF Conference on Computer Vision and Pattern Recognition*, pages 6229–6238, 2022. 7

[47] Noam Shazeer, Azalia Mirhoseini, Krzysztof Maziarz, Andy Davis, Quoc Le, Geoffrey Hinton, and Jeff Dean. Outrageously large neural networks: The sparsely-gated mixture-of-experts layer. *arXiv preprint arXiv:1701.06538*, 2017. 1, 2, 3, 4

[48] Sheng Shen, Le Hou, Yanqi Zhou, Nan Du, Shayne Longpre, Jason Wei, Hyung Won Chung, Barret Zoph, William Fedus, Xinyun Chen, et al. Flan-moe: Scaling instruction-finetuned language models with sparse mixture of experts. *arXiv preprint arXiv:2305.14705*, 2023. 2

[49] Mohammed Suhail, Carlos Esteves, Leonid Sigal, and Ameesh Makadia. Generalizable patch-based neural rendering. In *European Conference on Computer Vision*. Springer, 2022. 1, 6

[50] Mohammed Suhail, Carlos Esteves, Leonid Sigal, and Ameesh Makadia. Generalizable patch-based neural rendering. *arXiv preprint arXiv:2207.10662*, 2022. 2, 3

[51] Cheng Sun, Min Sun, and Hwann-Tzong Chen. Direct voxel grid optimization: Super-fast convergence for radiance fields reconstruction. In *Proceedings of the IEEE/CVF Conference*

11

on *Computer Vision and Pattern Recognition*, pages 5459–5469, 2022. 1

[52] Cheng Sun, Min Sun, and Hwann-Tzong Chen. Direct Voxel Grid Optimization: Super-Fast Convergence for Radiance Fields Reconstruction. In *Proceedings of the IEEE/CVF Conference on Computer Vision and Pattern Recognition*, pages 5459–5469, 2022. 2

[53] Mukund Varma T, Peihao Wang, Xuxi Chen, Tianlong Chen, Subhashini Venugopalan, and Zhangyang Wang. Is attention all that neRF needs? In *The Eleventh International Conference on Learning Representations*, 2023. 1, 2, 3, 4, 6, 7, 9

[54] Matthew Tancik, Vincent Casser, Xinchen Yan, Sabeek Pradhan, Ben Mildenhall, Pratul P Srinivasan, Jonathan T Barron, and Henrik Kretzschmar. Block-nerf: Scalable large scene neural view synthesis. In *Proceedings of the IEEE/CVF Conference on Computer Vision and Pattern Recognition*, pages 8248–8258, 2022. 3

[55] Alex Trevithick and Bo Yang. Grf: Learning a general radiance field for 3d representation and rendering. In *Proceedings of the IEEE/CVF International Conference on Computer Vision*, pages 15182–15192, 2021. 2

[56] Huan Wang, Jian Ren, Zeng Huang, Kyle Olszewski, Menglei Chai, Yun Fu, and S. Tulyakov. R2L: Distilling Neural Radiance Field to Neural Light Field for Efficient Novel View Synthesis. In *European Conference on Computer Vision*. Springer, Springer, 2022. 2

[57] Peihao Wang, Zhiwen Fan, Tianlong Chen, and Zhangyang Wang. Neural implicit dictionary learning via mixture-of-expert training. In *International Conference on Machine Learning*, pages 22613–22624. PMLR, 2022. 3

[58] Qianqian Wang, Zhicheng Wang, Kyle Genova, Pratul P Srinivasan, Howard Zhou, Jonathan T Barron, Ricardo Martin-Brualla, Noah Snavely, and Thomas Funkhouser. Ibrnet: Learning multi-view image-based rendering. In *Proceedings of the IEEE/CVF Conference on Computer Vision and Pattern Recognition*, pages 4690–4699, 2021. 1, 2, 6, 7

[59] Xin Wang, Fisher Yu, Lisa Dunlap, Yi-An Ma, Ruth Wang, Azalia Mirhoseini, Trevor Darrell, and Joseph E Gonzalez. Deep mixture of experts via shallow embedding. In *Uncertainty in artificial intelligence*, pages 552–562. PMLR, 2020. 3

[60] Zhou Wang, Alan C Bovik, Hamid R Sheikh, and Eero P Simoncelli. Image quality assessment: from error visibility to structural similarity. *IEEE transactions on image processing*, 13(4):600–612, 2004. 6

[61] Suttisak Wizadwongsa, Pakkapon Phongthawee, Jiraphon Yenphraphai, and Supasorn Suwajanakorn. Nex: Real-time view synthesis with neural basis expansion. In *IEEE Conference on Computer Vision and Pattern Recognition (CVPR)*, 2021. 1

[62] Suttisak Wizadwongsa, Pakkapon Phongthawee, Jiraphon Yenphraphai, and Supasorn Suwajanakorn. Nex: Real-time view synthesis with neural basis expansion. In *Proceedings of the IEEE/CVF Conference on Computer Vision and Pattern Recognition*, pages 8534–8543, 2021. 6, 7, 13

[63] Wenqi Xian, Jia-Bin Huang, Johannes Kopf, and Changil Kim. Space-time neural irradiance fields for free-viewpoint video. In *Proceedings of the IEEE/CVF Conference on Computer Vision and Pattern Recognition*, pages 9421–9431, 2021. 2

[64] Dejia Xu, Yifan Jiang, Peihao Wang, Zhiwen Fan, Humphrey Shi, and Zhangyang Wang. SinNeRF: Training Neural Radiance Fields on Complex Scenes From a Single Image. *ArXiv Preprint ArXiv:2204.00928*, 2022. 1

[65] Dejia Xu, Yifan Jiang, Peihao Wang, Zhiwen Fan, Yi Wang, and Zhangyang Wang. Neurallift-360: Lifting an in-the-wild 2d photo to a 3d object with 360deg views. In *Proceedings of the IEEE/CVF Conference on Computer Vision and Pattern Recognition*, pages 4479–4489, 2023. 1

[66] Brandon Yang, Gabriel Bender, Quoc V Le, and Jiquan Ngiam. Condconv: Conditionally parameterized convolutions for efficient inference. *Advances in Neural Information Processing Systems*, 32, 2019. 3

[67] Xingyi Yang, Jingwen Ye, and Xinchao Wang. Factorizing knowledge in neural networks. In *European Conference on Computer Vision*, 2022. 2

[68] Xingyi Yang, Daquan Zhou, Songhua Liu, Jingwen Ye, and Xinchao Wang. Deep model reassembly. In *Advances in Neural Information Processing Systems*, 2022. 2

[69] Yao Yao, Zixin Luo, Shiwei Li, Tian Fang, and Long Quan. Mvsnet: Depth inference for unstructured multi-view stereo. In *Proceedings of the European conference on computer vision (ECCV)*, pages 767–783, 2018. 1

[70] Alex Yu, Vickie Ye, Matthew Tancik, and Angjoo Kanazawa. pixelnerf: Neural radiance fields from one or few images. In *Proceedings of the IEEE/CVF Conference on Computer Vision and Pattern Recognition*, pages 4578–4587, 2021. 1, 2, 6, 7

[71] Seniha Esen Yuksel, Joseph N. Wilson, and Paul D. Gader. Twenty years of mixture of experts. *IEEE Transactions on Neural Networks and Learning Systems*, 23(8):1177–1193, 2012. 2

[72] Kai Zhang, Gernot Riegler, Noah Snavely, and Vladlen Koltun. NeRF++: Analyzing and improving neural radiance fields. *arXiv preprint arXiv:2010.07492*, 2020. 7

[73] Richard Zhang, Phillip Isola, Alexei A Efros, Eli Shechtman, and Oliver Wang. The unreasonable effectiveness of deep features as a perceptual metric. In *Proceedings of the IEEE conference on computer vision and pattern recognition*, pages 586–595, 2018. 6

[74] Zelin Zhao and Jiaya Jia. End-to-end view synthesis via nerf attention. *arXiv preprint arXiv:2207.14741*, 2022. 2

[75] Tinghui Zhou, Richard Tucker, John Flynn, Graham Fyffe, and Noah Snavely. Stereo magnification: Learning view synthesis using multiplane images. *arXiv preprint arXiv:1805.09817*, 2018. 6

[76] Yanqi Zhou, Tao Lei, Hanxiao Liu, Nan Du, Yanping Huang, Vincent Zhao, Andrew Dai, Zhifeng Chen, Quoc Le, and James Laudon. Mixture-of-experts with expert choice routing. *arXiv preprint arXiv:2202.09368*, 2022. 2

[77] Simiao Zuo, Xiaodong Liu, Jian Jiao, Young Jin Kim, Hany Hassan, Ruofei Zhang, Tuo Zhao, and Jianfeng Gao. Taming sparsely activated transformer with stochastic experts. *arXiv preprint arXiv:2110.04260*, 2021. 2, 4

S1. More Training / Inference Details

The base learning rates for the feature extraction network and GNT-MOVE are 10^{-3} and 5×10^{-4}, respectively, which decay exponentially over training steps. For the zero-shot generalization experiments, we train the network for 330,000 steps with 4096 rays sampled from 4 different views in each iteration. In the few-shot setting, we further fine-tune the pretrained model on each scene for 2,4000 steps. During the inference, we sample 192 coarse points per ray in all experiments.

S2. Cross-Scene Generalization

S2.1. Testing Datasets

Local Light Field Fusion (LLFF) [33] consists of 8 forward-facing captures of real-world scenes using a smartphone. NeRF Synthetic dataset [34] consists of 8, 360° scenes of objects with complicated geometry and realistic material. Each scene consists of images rendered from viewpoints randomly sampled on a hemisphere around the object. Shiny-6 dataset [62] contains 8 forward-facing scenes with challenging view-dependent optical effects, such as the rainbow reflections on a CD, and the refraction through liquid bottles. Tanks-and-Temples [42] is a complex outdoor dataset and contains large unbounded scenes. Following NeRF++, we evaluate on four scenes, including M60, Train, Truck, and Playground, and use the same evaluate views as NeRF++ does. NMR [24] contains 360° views of various objects from unseen categories, which could be downloaded from NMR_Dataset.zip[2] (hosted by the authors of Differentiable Volumetric Rendering [36]). In the main paper, we report the average metrics across all eight scenes on each dataset for cross-scene generalization experiments.

S2.2. Per-Scene Breakdown Results for Zero-Shot Generalization

To better demonstrate the effectiveness of our customized MoE, in Table S2 and Table S3, we pick a few representative scenes for breakdown analysis of both GNT's and GNT-MOVE's quantitative results presented in Table 1a in the main paper. The scenes we choose mainly cover the complex geometries (e.g., leaves and orchids) and materials (e.g., room and materials). In both tables, our GNT-MOVE outperforms GNT by a significant margin in most scenes and achieves comparable results in the rest ones, demonstrating that with necessary customizations, MoE could be a strong tool to push the frontier of generalizable NeRF.

It is also worth mentioning that in Table S3, our GNT-MOVE has demonstrated superior performance, especially in scenes with complex materials (*e.g.*, Drums, Materials,

Ship), showing that the customized MoE further enables cross-scene NeRF to generalize to difficult scenarios.

S2.3. More Expert Selection Analyses

In Figure S1, we visualize more unseen scene rendering results and also the corresponding expert selections in the format of expert maps. It can be observed that our customized MoE is not only capable of keeping consistent selection across scenes (*e.g.*, white background in the left three scenes, leaves in the right two scenes), but also reacts properly to complex lighting effects and materials (*e.g.*, sparkling water in the left bottom scene Ship).

S3. More Comparison: GNT v.s. GNT-MOVE

While the model size/speed is indeed not the main focus in this paper, GNT-MoE does generalize better, than the non-MoE counterpart with even heavier parameterization, while keeping per-instance inference low-cost.

Below, ▷ **1)** and ▷ **2)** demonstrate that the solid gain of MoE for generalizable NeRF goes way beyond naively larger model size; and ▷ **3)** demonstrates that the gain can only be unleashed with PE and SR. Detailed results could be found in Table S1. As preliminary, every expert in GNT-MOVE is half the size of GNT's same layer. The default GNT-MOVE (row 4) selects E = 2 such experts from K = 4 candidates, plus 1 permanent expert. Hence, if we treat the total parameter and inference FLOPs of GNT both as unit (**"1"**), then the default GNT-MOVE has **"2.5"** total parameter and **"1.5"** inference FLOPs. We construct the following comparison groups:

▷ **1) the same FLOPs at inference.** Rows 1-2 compare GNT (FLOPs **"1"**) versus GNT-MOVE using only one selectable expert (E = 1) + one PE (0.5 + 0.5 = **"1"**). Despite the same inference complexity, the extra flexibility to "select" endows GNT-MOVE with superior performance.

▷ **2) the same total parameter.** Row 3 widens GNT by 2.5 times to match the total parameter size **"2.5"** of GNT-MOVE, called "GNT (Large)". Compared to Row 4 (default GNT-MOVE), they have the same total parameter counts; meanwhile, GNT-MOVE has smaller per-inference FLOPs. However, GNT (Large) performs worse - and that clearly indicates for generalizable NeRF, "the more parameter the better" is NOT the right quote, and per-scene specialization is necessary.

▷ **3) Does PE undermine MoE claim? NO.** First, the above two points already justified the necessity of MoE and disapprove "natural to have better performance with more parameters". Second, our core claim is NEVER "MoE shall work out of box for NeRF". Instead, while MoE is promising to balance "generality" and "specialization", making it work for generalizable NeRF demands customized tactics to inject the key priors of cross-view consistency & cross-scene commodity - PE is one such tactic.
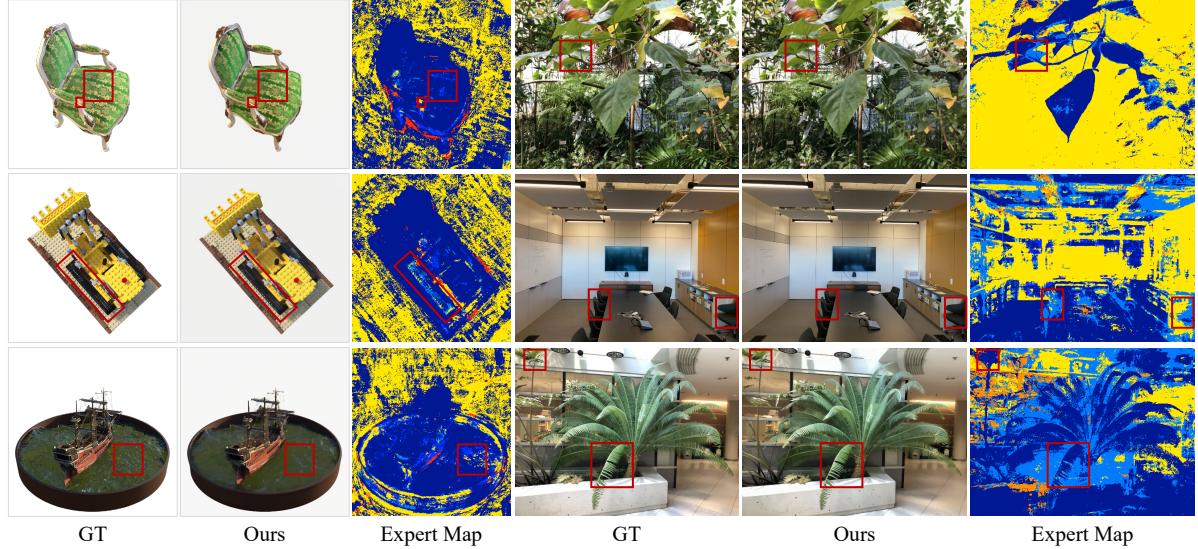
Figure S1: Results of unseen scene rendering and visualization of expert selection using different colors.

Models	Local Light Field Fusion (LLFF)				NeRF Synthetic				Tanks-and-Temples (Truck)		
	PSNR↑	SSIM↑	LPIPS↓	Avg↓	PSNR↑	SSIM↑	LPIPS↓	Avg↓	PSNR↑	SSIM↑	LPIPS↓
GNT	25.86	0.867	0.116	0.047	27.29	0.937	0.056	0.030	17.39	0.561	0.429
GNT-MOVE (E=1, K=4, w. PE)	25.94	0.868	0.111	0.043	27.43	0.939	0.057	0.029	19.08	0.611	0.393
GNT (Large)	25.89	0.867	0.113	0.046	27.37	0.936	0.058	0.033	18.26	0.579	0.405
GNT-MOVE (E=2, K=4, w. PE)	**26.02**	**0.869**	**0.108**	**0.043**	**27.47**	**0.940**	**0.056**	**0.029**	**19.71**	**0.628**	**0.379**
GNT-MOVE **w.o. PE** (E=3, K=5)	25.81	0.867	0.114	0.047	27.32	0.933	0.059	0.031	18.11	0.570	0.414

Table S1: Comparisons to illustrate the solid gain of MoE and PE in GNT-MOVE.

Models	Room	Leaves	Orchids	Flower	T-Rex	Horns
GNT	29.63	19.98	18.84	25.86	24.56	26.34
Ours	**29.94**	**20.45**	**19.38**	**27.04**	**24.58**	**26.87**

(a) PSNR↑

Models	Room	Leaves	Orchids	Flower	T-Rex	Horns
GNT	0.940	0.756	0.661	0.859	0.885	0.892
Ours	**0.946**	**0.770**	**0.668**	**0.871**	0.878	**0.894**

(b) SSIM↑

Models	Room	Leaves	Orchids	Flower	T-Rex	Horns
GNT	0.091	0.183	0.216	0.108	0.127	0.118
Ours	**0.087**	**0.173**	**0.209**	**0.101**	**0.123**	**0.113**

(c) LPIPS↓

Models	Room	Leaves	Orchids	Flower	T-Rex	Horns
GNT	0.031	0.097	0.119	0.048	0.054	0.046
Ours	**0.029**	**0.093**	**0.115**	**0.043**	**0.054**	**0.044**

(d) Avg↓

Table S2: Comparison between our GNT-MOVE and GNT for cross-scene generalization under zero-shot setting on the LLFF Dataset (scene-wise).

Models	Chair	Drums	Materials	Mic	Ship
GNT	29.17	22.83	23.80	29.61	25.99
Ours	**29.64**	**23.19**	**24.16**	**30.30**	**26.48**

(a) PSNR↑

Models	Chair	Drums	Materials	Mic	Ship
GNT	0.959	0.927	0.931	0.977	0.836
Ours	**0.962**	**0.979**	**0.935**	**0.982**	**0.845**

(b) SSIM↑

Models	Chair	Drums	Materials	Mic	Ship
GNT	0.038	0.059	0.058	0.017	0.154
Ours	**0.038**	**0.057**	**0.056**	**0.015**	**0.149**

(c) LPIPS↓

Models	Chair	Drums	Materials	Mic	Ship
GNT	0.021	0.044	0.040	0.014	0.054
Ours	**0.021**	**0.042**	**0.040**	**0.013**	**0.051**

(d) Avg↓

Table S3: Comparison between our GNT-MOVE and GNT for cross-scene generalization under zero-shot setting on the NeRF Synthetic Dataset (scene-wise).

To explain the second note, we stress that learning MoEs over NeRFs differs greatly from over standard image sets. If treating each view observation as an image sample, a "NeRF dataset" would exhibit significant clustering due to different views of the same scene, and even different scenes will bear natural scene similarity. The highly non-i.i.d distribution, with multi-dimensional similarity entangled across views and scenes, can make naive MoE training more prone to collapse - see our ablation in Supplement sec. 3. Our important contribution is to show one can reap the benefit of MoE with proper regularizations including PE.

To directly show PE values beyond just "more parameters", we compare Row 5 in Table (replacing GNT-MOVE's PE with a selectable expert, and making $E = 3$), which has same total parameter & inference FLOPs with our default GNT-MOVE setting (Row 4). Having PE helps evidently.